

Energy & Environmental Science

Accepted Manuscript



This is an *Accepted Manuscript*, which has been through the Royal Society of Chemistry peer review process and has been accepted for publication.

Accepted Manuscripts are published online shortly after acceptance, before technical editing, formatting and proof reading. Using this free service, authors can make their results available to the community, in citable form, before we publish the edited article. We will replace this *Accepted Manuscript* with the edited and formatted *Advance Article* as soon as it is available.

You can find more information about *Accepted Manuscripts* in the [Information for Authors](#).

Please note that technical editing may introduce minor changes to the text and/or graphics, which may alter content. The journal's standard [Terms & Conditions](#) and the [Ethical guidelines](#) still apply. In no event shall the Royal Society of Chemistry be held responsible for any errors or omissions in this *Accepted Manuscript* or any consequences arising from the use of any information it contains.

**Achieving overall water splitting using titanium dioxide-based photocatalysts of
different phases**

Rengui Li¹, Yuxiang Weng², Xin Zhou¹, Xiuli Wang¹, Yang Mi^{2,3}, Ruifeng Chong^{1,3},
Hongxian Han¹ and Can Li^{1*}

1. *State Key Laboratory of Catalysis, Dalian Institute of Chemical Physics, Chinese Academy of Sciences, Dalian National Laboratory for Clean Energy, Zhongshan Road 457, Dalian, 116023, China.*
2. *The Key Laboratory of Softmatter Physics, The Institute of Physics, Chinese Academy of Sciences, Beijing 100190, China.*
3. *University of Chinese Academy of Sciences, Beijing, 100049, China.*

*Corresponding author: Prof. Can Li, canli@dicp.ac.cn

Abstract.

Titanium dioxide (TiO₂) is regarded as the benchmark semiconductor in photocatalysis, which possesses a suitable band structure and makes the overall water splitting reaction thermodynamically possible. However, photocatalytic overall water splitting (POWS) ($2H_2O \rightarrow 2H_2 + O_2$) can only take place on rutile but hardly on anatase and brookite TiO₂. So achieving the POWS on TiO₂-based photocatalysts has remained a long-standing challenge for over 40 years. In this work, we found that the POWS on anatase and brookite TiO₂ becomes feasible under prolonged UV light irradiation. Further investigation by means of electron spin resonance spectra (EPR) and transient infrared absorption-excitation energy scanning spectrum (TRIRA-ESS) reveals that both kinetics and thermodynamics factors contributed to unique POWS activity for different phases of TiO₂. Kinetically the process of photocatalysis differs on different phases of TiO₂ due to the intermediates (OH radical for anatase and brookite TiO₂, peroxy species for rutile TiO₂) that are formed. Thermodynamically there are many trapped states lying near the valence band of anatase and brookite but not for rutile TiO₂, which reduce the overpotential for water oxidation. These findings develop our understanding of why some semiconductors are inactive as POWS photocatalysts despite having thermodynamically suitable band structures for the proton reduction and water oxidation reactions.

Keywords: Photocatalysis, overall water splitting, TiO₂, water oxidation.

Solar hydrogen production using photocatalytic water splitting is regarded as a promising strategy for harnessing solar energy to supply hydrogen energy.^{1,2} Titanium dioxide (TiO₂) is a popular and standard semiconductor used in photocatalysis, and exists in three common crystalline structures, anatase, rutile and brookite, that have been extensively investigated. Generally, anatase TiO₂ is recognized as the most active phase in photocatalysts for environmental applications, while rutile and brookite TiO₂ are seldom considered.³⁻⁶ In the past few decades, almost all the researches on TiO₂ can only obtain H₂ but no O₂ was detected during photocatalytic overall water splitting although it has thermodynamic feasible band structure. In the photocatalytic overall water splitting reaction (POWS, $2H_2O \rightarrow 2H_2 + O_2$), H₂ and O₂ should be produced simultaneously with H₂/O₂ stoichiometric ratio of 2.0, which has been achieved in photoelectrochemical (PEC) system using TiO₂ photoanode as early as 1972.⁷ However, it has seldom been achieved on TiO₂-based nanoparticulate photocatalyst. This challenge persists despite the fact that TiO₂ has suitable band structure for both proton reduction and water oxidation under UV light irradiation. Besides, a similar phenomenon has been observed for other popular photocatalysts (e.g., Ta₃N₅, TaON). That is, some photocatalysts have suitable band structures that are thermodynamically feasible for POWS, yet they fail to catalyze POWS reaction.

Immense efforts have been made to achieve POWS on TiO₂ previously. The introduction of some inorganic ions (e.g., Cl⁻, CO₃²⁻) has been reported to somewhat improve the stoichiometric production of H₂ and O₂, which might be attributed to the intermediates involving the ions (e.g., C₂O₄²⁻, ClO⁻) that are formed in these systems.^{8,9}

Recently, it was reported that the POWS can only take place on rutile but not on anatase TiO₂.¹⁰ Nevertheless, the intrinsic reason for this observation remains unknown. In addition, the water splitting mechanism, especially the mechanism of water oxidation on TiO₂-based photocatalysts are quite controversial in the literature.^{5,11-18}

Herein, we reported our results that photocatalytic overall water splitting (POWS) reaction can take place on TiO₂-based photocatalysts with different phases (anatase, rutile and brookite) under the prolonged UV light irradiation. We found that the stable overall water splitting with stoichiometric H₂/O₂ ratio can be achieved on rutile TiO₂. However, anatase and brookite TiO₂ can only produce H₂ at the initial stage, but H₂ and O₂ are obtained simultaneously on after long time irradiation. Further investigations by means of electron spin resonance spectra (EPR), transient infrared absorption-excitation energy scanning spectrum (TRIRA-ESS) and DFT calculations reveal that both thermodynamics and kinetics contributed to unique POWS activity for different phases of TiO₂. Kinetically the process of photocatalysis differs on different phases of TiO₂ due to the intermediates (OH radical for anatase and brookite TiO₂, peroxy species for rutile TiO₂) that are formed. Thermodynamically there are many trapped states lying below the Fermi levels of anatase and brookite TiO₂ (but no trapped states can be found on rutile TiO₂), which can reduce the overpotential for water oxidation. Theoretical calculation has demonstrated that the most stable surface of anatase and rutile TiO₂ are (101) and (110) facets.^{19,20} Similar calculation method was also introduced for brookite TiO₂, which shows that (210) facet is the most stable facet (Figure S1 and Table S1). Firstly, anatase, rutile and brookite TiO₂ samples exposed

with (101), (110) and (210) facets were prepared according to the references.^{21,22} The as-prepared TiO₂ samples were demonstrated to be pure phases and well-crystallized by XRD and Raman characterization (Figure 1a and 1b, Figure S2). HRTEM images revealed that the most exposed crystal facets for anatase, rutile and brookite TiO₂ samples are (101), (110) and (210), respectively, indicating the stable surface structures of them are synthesized successfully (Figure 1c-1n).

Table 1 lists the POWS performance of the prepared different phases of TiO₂ samples under the irradiation of Xe lamp (the emission spectrum was shown in Figure S3). Only H₂, but no O₂, is detected for anatase TiO₂ indicating that the POWS reaction does not take place on the anatase TiO₂ (entries 1 and 2). However, both H₂ and O₂ are produced simultaneously on rutile TiO₂ with H₂/O₂ ratio close to 2.0, indicating that the POWS ($2H_2O \rightarrow 2H_2 + O_2$) is achieved (entries 3, 4 and 5). In addition, brookite TiO₂ (entries 6) shows similar performance with anatase TiO₂, namely, only H₂ can be achieved but without any O₂. Commercial TiO₂ samples were also investigated for comparison (entries 7 and 8). It can be found that only H₂ was produced for commercial anatase TiO₂, however, commercial rutile can obtain H₂ and O₂ simultaneously though the photoactivity is low. The similar results were also reported by using a series of commercial anatase and rutile TiO₂ from different supply corporations recently.²³ The above results clearly indicate that the POWS performance on TiO₂-based photocatalyst is closely related to its crystalline phases.

Photocatalytic H₂ or O₂ production reaction in the presence of CH₃OH (holes acceptor) or AgNO₃ (electrons acceptor) was also performed to further evaluate the performances

for TiO₂ samples (Figure S4). Anatase and brookite TiO₂ show comparable H₂ production performances, which is better than rutile TiO₂ in the presence of CH₃OH. However, rutile TiO₂ shows much better O₂ evolution performance than anatase and brookite TiO₂ when Ag⁺ was used as electron acceptor. The result shows the different reduction and oxidation ability for anatase, rutile and brookite TiO₂, which led us to the conclusion that the POWS on TiO₂ is highly dependent on the crystalline phase of the TiO₂, especially for the water oxidation reaction. This result also indicates that anatase and brookite TiO₂ exhibit the similar performance both for H₂ production and O₂ production half reactions.

To investigate the photogenerated holes for anatase or brookite TiO₂ during the proton reduction for H₂ production, a photocatalytic experiment under the prolonged UV light irradiation (light intensity, 1000mW/cm²) was carried out. As shown in Figure 2a, only H₂ without O₂ is produced in the initial stage for anatase TiO₂. In a subsequent experiment, the reaction system was then vacuumed and no O₂ was detected, but the H₂ production rate decreased. In the second cycle, H₂ production rate decreased and O₂ was still not detected. In the third cycle after the whole reaction time of more than 5 hours, small amount of oxygen was detected and maintained in the following cycles. The appearance of O₂ evolution after sufficient light irradiation is a surprising result. Figure 2b shows the results of rutile TiO₂ throughout several cycles of the reaction test. H₂ and O₂ production with a H₂/O₂ ratio close to 2.0 was always maintained. Interestingly, brookite TiO₂ shows the similar phenomenon with anatase TiO₂ (Figure 2c), namely, H₂ was only produced at the initial stage but O₂ was generated

simultaneously after the prolonged UV light irradiation. The phenomenon that anatase and brookite TiO_2 show similar performances for the POWS reaction could be ascribed to the similar atomic structure between brookite (210) of and anatase (101) facets.²⁴ It should be pointed out that all the samples in Table 1 were used in this experiment and the samples with the same phases show the similar performance. These results clearly indicate that the POWS to produce both H_2 and O_2 can be achieved not only for rutile TiO_2 but also for anatase and brookite TiO_2 . Notably, we found that O_2 can be produced on anatase and brookite TiO_2 after a prolonged UV irradiation during the photocatalytic reaction.

To understand why the different phases of TiO_2 perform differently as photocatalysts in the POWS reaction, we characterized major aspects of the issue, including carrier dynamics, kinetics and thermodynamics. Particularly, we focused on the differences of water oxidation for the different phases of TiO_2 .

The transient dynamics of the two commonly-used phases, anatase and rutile TiO_2 , were studied to probe the lifetimes of photoexcited holes. The lifetimes of the holes excited in rutile TiO_2 were found to be longer than those in anatase TiO_2 . However, in the presence of Pt cocatalyst, the lifetimes were almost the same for both anatase and rutile TiO_2 (shown in Figure S5a). It should be noted that the Pt was deposited as cocatalyst in all the POWS reactions for both anatase and rutile TiO_2 (without the Pt cocatalyst, no H_2 evolution is detected for either the anatase or rutile TiO_2). Thus, the dynamics of the photogenerated holes in the anatase and rutile TiO_2 are quite similar. To further clarify this point, Ag^+ (AgNO_3) was introduced as an electron acceptor to investigate

the behavior of the photoexcited holes, and again the lifetimes of the photoexcited holes were almost the same, indicating that the dynamics of the photogenerated holes for anatase and rutile TiO₂ are similar. Therefore, we can conclude that the initial dynamics of photogenerated holes are not responsible for the behaviors of the different phases of TiO₂ in POWS.

To further explore the different oxygen-containing intermediate on different phases of TiO₂ samples, we employed the EPR spin-trap technique to probe the reactive oxygen species derived on the surface of TiO₂ under light irradiation. Firstly, we performed the EPR experiment for all three TiO₂ samples with DMPO (dimethyl pyridine N-oxide) as electron trapping agent under the atmosphere of Ar (Figure 3). No signal was detected in the dark but totally different signals for three TiO₂ samples were obtained under light irradiation. For anatase TiO₂, four characteristic peaks are obviously observed and the standard ratios of peak intensities are 1:2:2:1, which can be ascribed to ·DMPO-OH.^{13,17,25} In addition, brookite TiO₂ shows almost the same EPR signal with anatase TiO₂, which is in good agreement with their similar photocatalytic performances. However, for rutile TiO₂, a typical seven-line paramagnetic signal is detected, which can be ascribed to ·DMPO-X as reported.²⁶⁻²⁸ We can infer that it is generated from the oxidation of DMPO by peroxide. It was also reported that peroxy species may serve as the reaction intermediates for the water oxidation on rutile TiO₂.¹¹⁻¹³ Valdes et al reported that peroxy species can be easily decomposed to O₂ by DFT calculations and conclude that this reaction step is the most favored step on rutile in water oxidation reaction.¹⁸ So we can speculate that the peroxy species can be easily decomposed to

produce O_2 on rutile. However, for anatase and brookite TiO_2 , the formed $\cdot OH$ radical may be strongly absorbed on the surface and coupled to evolve O_2 after saturation of absorption. The different oxygen-containing intermediates formed on anatase and rutile TiO_2 can also be demonstrated by the diversity of surface hydroxyl oxygen of TiO_2 before and after the reaction^{29,30} (Figures S6 and S7). It was found that the proportion of hydroxyl oxygen for anatase TiO_2 was obviously increased after UV light irradiation (from 5.0% to 9.7%) but remained almost unchanged for rutile TiO_2 . Thus, the peroxy species are the most likely oxygen-containing intermediate derived from water oxidation on rutile TiO_2 while $\cdot OH$ radical species are preferring to prevail from water oxidation on anatase TiO_2 . Our EPR results suggest that different intermediates are really formed during the photocatalytic water splitting for three kinds of TiO_2 samples (peroxy species for rutile TiO_2 , $\cdot OH$ radical for anatase and brookite TiO_2). The different intermediates resulted in different surface reaction processes, which mainly contribute to the kinetics for POWS on TiO_2 -based photocatalysts.

EPR experiments without electron trapping agent were also conducted under the Ar atmosphere. Figure 4 shows the EPR results with and without UV light irradiation. The red-line signals were collected after 20 min UV light irradiation and then the sample tubes were quickly transferred for detection. No signals were detected for rutile TiO_2 regardless of dark or light irradiation. However, anatase TiO_2 shows an obvious EPR signal at $g=1.9998$, which could be ascribed to $O^{\cdot -}$.^{31,32} A weak signal at $g=1.9890$ could be ascribed to the unsaturated Ti^{3+} .^{31,33,34} The signal of $O^{\cdot -}$ became stronger after the UV light irradiation, indicating that part of O^{2-} in the lattice could be oxidized to $O^{\cdot -}$ by

photoexcited holes during the photocatalytic reaction. For brookite TiO_2 , no signal was detected under dark condition while a strong EPR signal at $g=1.9998$, which is ascribed to O^- similar to anatase TiO_2 . Interestingly, the signals at $g=1.9890$ and $g=1.9621$ were only achieved on brookite TiO_2 , which are ascribed to the unsaturated Ti^{3+} . The presence of Ti^{3+} under light irradiation most possibly contributes to the non-stoichiometric ratio of H_2/O_2 for anatase and brookite TiO_2 because partial photoexcited holes are participating in oxidizing the lattice oxygen to the observed O^- .

To further investigate the thermodynamics for different POWS performances on TiO_2 -based photocatalysts, different phases of TiO_2 were also characterized by the recent reported transient infrared absorption-excitation energy scanning spectrum (TRIRA-ESS), which can identify deep trapped electron energy levels above the valence band (VB) but below the Fermi level of the trapped electrons, the corresponding integrated density of the states, and the shallow trapping energy level below the conduction band.^{35,36} The TRIRA-ESS results shown in Figure 5a can be divided into two regions: one below the Fermi-level of the trapped electrons (i.e., from 0 to 1.79 eV) arising from the trapping states above the VB, and another region above the Fermi-level of the trapped electrons but below the conduction band (CB) originating from the shallow trapping states. There are remarkable differences between anatase and rutile TiO_2 in the region below the Fermi-level of the trapped electrons (denoted as E_{fs} , which is different from Fermi level of free electrons in the CB denoted as E_{fn} ³⁷), namely, there are deep trapped states obviously observed in the anatase TiO_2 that are not present in the rutile TiO_2 . The TRIRA-ESS for brookite TiO_2 was also performed, which shows the similar

deep trapped states with anatase TiO₂ (Figure S8). It can be speculated that the lack of O₂ evolution for anatase and brookite TiO₂ in the initial stage of the reaction is possibly due to the trapped states that are present in the bulk and surface regions. These states could reduce the overpotential for water oxidation.

Because the photocatalytic performance of anatase TiO₂ changed after long exposure to UV light irradiation, anatase TiO₂ film was pre-treated under different conditions for TRIRA-ESS characterization. As shown in Figure 5b, the trapped states with their energy levels close to the VB are nearly unchanged after saturated with water vapor, only the integrated densities of states are slightly increased. However, when anatase TiO₂ was treated with UV-laser irradiation, the trapped states were completely removed within the scanning excitation laser wavelength indicating that light irradiation can indeed change the deep trapped states near the VB of anatase TiO₂. Furthermore, we also conducted the Mott-Schottky analysis for all three kinds of TiO₂ before and after the UV light irradiation, indicating that the conduction band (CB) positions of them were not changed after the light treatment (Figure S9). From the TRIRA-ESS study, we can conclude that the deep trapped states can only be detected for anatase TiO₂ and UV-laser irradiation can remove the deep trapped states, which is corresponding to the unique photocatalytic performance for anatase TiO₂.

To confirm the above results, we conducted photocatalytic water oxidation with anatase and rutile TiO₂ pre-treated under UV light irradiation. Anatase and rutile TiO₂ were first irradiated for different time and then used for water oxidation reactions using AgNO₃ as the electron acceptor. As listed in Table S2, anatase TiO₂ shows a remarkable

enhancement in O_2 evolution with increasing irradiation time. In fact, the photocatalytic O_2 evolution activity of anatase TiO_2 pre-irradiated for 8 hours shows 4 times of that the untreated sample (entries 1, 2 and 3). However, rutile TiO_2 shows nearly no difference regardless of the irradiation time (entries 4, 5 and 6). It indicates that the trapped states in anatase TiO_2 can be quenched by light irradiation, consequently resulting in the different performances for water oxidation, which is in good agreement with the TRIRA-ESS result.

Based on the above results, we can conclude that the existence of deep trapped states near the VB level of TiO_2 is directly responsible for the POWS behaviors for different phases of TiO_2 . A schematic description of deep trapped states for anatase and rutile TiO_2 is shown in Figure 5c. A plausible explanation is that the deep trapped states located above the VB of anatase TiO_2 can reduce the potential of photogenerated holes that are produced during the photocatalytic reaction. However, when these trapped states are gradually removed by UV light irradiation, the overpotential for water oxidation is increased and O_2 is produced subsequently. However, the rutile TiO_2 samples does not have trapped states above the VB level, so that it has enough potential to drive the proton reduction and water oxidation reactions even without light treatment. It should be pointed out that although the photocatalytic water oxidation on TiO_2 can be ascribed to both thermodynamics and kinetics, both of which are closely related but not separated to each other. The presence of deep trapped states near the valence band of anatase and brookite TiO_2 reduce the overpotential for water oxidation, so that the photogenerated holes are more preferable to oxidizing H_2O molecule to produce the

OH radical. This process is a 2-electron-process, which requires less potential than a 4-electron-process to produce O_2 directly. The UV light with high intensity can gradually reduce the deep trapped states near the valence band of anatase and brookite TiO_2 , so that the overpotential for water oxidation is increased, and simultaneously lead to the result that H_2O can be oxidation by the 4-electron-process to produce O_2 .

A DFT calculation was also conducted to simulate the water oxidation process on anatase, rutile and brookite TiO_2 (Figure S10). The adsorption energy of H_2O onto the anatase (101) surface is calculated to be 0.55 eV, and the first O-H dissociation energy is endothermic by 0.34 eV with a barrier of 0.73 eV. As for the product of this step, the H atom is adsorbed onto the O_{2c} atom, and the OH group is left to attach to the Ti_{5c} atom to form a surface-adsorbed hydroxyl radical. The second O-H dissociation step to produce an O atom is predicted to be endothermic by 0.43 eV, with a barrier of 0.62 eV. For the molecular adsorption of water onto the rutile (110) surface, the calculated adsorption energy for H_2O is exothermic by 0.73 eV, and the first O-H dissociation energy is 0.14 eV with a low barrier of 0.23 eV. The second O-H dissociation step is computed to be exothermic by 0.36 eV, with a barrier of 0.45 eV. The calculated adsorption energy for H_2O onto the brookite (210) surface is exothermic by 0.36 eV, and the first O-H dissociation energy is 0.25 eV. All the energies on brookite (210) are larger than rutile (110) surface, which may be attributed to the different photocatalytic performances for them. The theoretical calculation results suggest that the water decomposition reaction on the rutile (110) surface is more favorable than that on the anatase (101) and brookite (210) surfaces both thermodynamically and kinetically.

It is worth noting that the surface structures of photocatalysts may be reconstructed under light irradiation. It was reported that anatase TiO_2 will form a disordered layer with two monolayer thickness by the irradiation of high intensity UV light.³⁸ Therefore, it is possible that the surfaces of anatase and brookite TiO_2 may be reconstructed to a quasi-rutile phase surface after prolonged irradiation, which would not only make less trapping states and improve the capability of water oxidation, but also produce more stable and favorable intermediates for the activation of H_2O molecule.

In conclusion, we report the POWS reaction can take place on rutile but hardly on anatase and brookite TiO_2 . However, the POWS on anatase and brookite TiO_2 become feasible under prolonged UV light irradiation. The POWS performances for different phases of TiO_2 are determined by both kinetics and thermodynamics. Kinetically the process of photocatalysis differs on different phases of TiO_2 due to the intermediates (OH radical for anatase and brookite TiO_2 , peroxy species for rutile TiO_2) that are formed. Thermodynamically there are many trapped states lying near the VB of anatase and brookite TiO_2 , which reduce the overpotential for water oxidation. These trapped states can be gradually removed by the irradiation of high intensity UV light, such that the POWS reaction can take place finally. Our work will be instructive for understanding the mechanisms for photocatalytic water splitting and shed light on why many semiconductors cannot achieve the POWS despite having thermodynamically suitable band structures for proton reduction and water oxidation reactions.

Acknowledgement.

This work was financially supported by the National Natural Science Foundation of China (NSFC Grant No. 21090340) and the 973 National Basic Research Program of the Ministry of Science and Technology (Grant 2014CB239400). The authors would like to thank Prof. James. R. Durrant at ICL for useful discussions.

References.

- 1 K. Maeda, T. Takata, M. Hara, N. Saito, Y. Inoue, H. Kobayashi, K. Domen, *J. Am. Chem. Soc.* **2005**, *127*, 8286-8287.
- 2 Y. Ma, X. Wang, Y. Jia, X. Chen, H. Han, C. Li, *Chem. Rev.* **2014**, *114*, 9987-10043.
- 3 R. L. Pozzo, M. A. Baltanas, A. E. Cassano, *Catal. Today* **1997**, *39*, 219-231.
- 4 D. Y. Goswami, *J. Solar Energy Eng.* **1997**, *119*, 101-107.
- 5 A. L. Linsebigler, G. Lu, J. T. Yates Jr, *Chem. Rev.* **1995**, *95*, 735-758.
- 6 O. Legrini, E. Oliveros, A. Braun, *Chem. Rev.* **1993**, *93*, 671-698.
- 7 A. Fujishima, *Nature* **1972**, *238*, 37-38.
- 8 K. Sayama, H. Arakawa, *J. Chem. Soc., Faraday Trans.* **1997**, *93*, 1647-1654.
- 9 L. Huang, R. Li, R. Chong, G. Liu, J. Han, C. Li, *Catal. Sci. Technol.* **2014**, *4*, 2913-2918.
- 10 K. Maeda, *Chem. Commun.* **2013**, *49*, 8404-8406.
- 11 R. Nakamura, A. Imanishi, K. Murakoshi, Y. Nakato, *J. Am. Chem. Soc.* **2003**, *125*, 7443-7450.
- 12 R. Nakamura, Y. Nakato, *J. Am. Chem. Soc.* **2004**, *126*, 1290-1298.
- 13 R. Nakamura, T. Okamura, N. Ohashi, A. Imanishi, Y. Nakato, *J. Am. Chem. Soc.* **2005**, *127*, 12975-12983.
- 14 P. Salvador, *J. Electrochem. Soc.* **1981**, *128*, 1895-1900.
- 15 P. Salvador, *J. Phys. Chem. C* **2007**, *111*, 17038-17043.
- 16 P. Salvador, C. Gutierrez, *J. Phys. Chem.* **1984**, *88*, 3696-3698.
- 17 Y. Nosaka, S. Komori, K. Yawata, T. Hirakawa, A. Y. Nosaka, *Phys. Chem. Chem. Phys.* **2003**, *5*, 4731-4735.
- 18 A. Valdes, Z.-W. Qu, G.-J. Kroes, J. Rossmeisl, J. K. Nørskov, *J. Phys. Chem. C* **2008** *112*, 9872-9879.
- 19 M. Lazzeri, A. Vittadini, A. Selloni, *Phys. Rev. B* **2001**, *63*, 155409.
- 20 H. Perron, C. Domain, J. Roques, R. Drot, E. Simoni, H. Catalette, *Theor. Chem. Acc.* **2007**, *117*, 565-574.
- 21 R. Chong, J. Li, X. Zhou, Y. Ma, J. Yang, L. Huang, H. Han, F. Zhang, C. Li, *Chem. Commun.* **2013**, *50*, 165-167.
- 22 H. Lin, L. Li, M. Zhao, X. Huang, X. Chen, G. Li, R. Yu, *J. Am. Chem. Soc.* **2012**, *134*, 8328-8331.

- 23 K. Maeda, *Chem. Commun.* **2013**, *49*, 8404-8406.
- 24 G. Liu, H. G. Yang, J. Pan, Y. Q. Yang, G. Q. Lu, H.-M. Cheng, *Chem. Rev.* **2014**, *114*, 9559-9612.
- 25 T. Hirakawa, Y. Nosaka, *Langmuir* **2002**, *18*, 3247-3254.
- 26 V. Brezova, D. Dvoranova, A. Staško, *Res. Chem. Inter.* **2007**, *33*, 251-268.
- 27 F. A. Villamena, J. K. Merle, C. M. Hadad, J. L. Zweier, *J. Phys. Chem. A* **2005**, *109*, 6089-6098.
- 28 J. Yu, J. Chen, C. Li, X. Wang, B. Zhang, H. Ding, *J. Phys. Chem. B* **2004**, *108*, 2781-2783.
- 29 X. Yang, C. Salzmann, H. Shi, H. Wang, M. L. Green, T. Xiao, *J. Phys. Chem. A* **2008**, *112*, 10784-10789.
- 30 R. Li, H. Kobayashi, J. Guo, J. Fan, *Chem. Commun.* **2011**, *47*, 8584-8586.
- 31 T. Berger, M. Sterrer, O. Diwald, E. Knözinger, D. Panayotov, T. Thompson, J. Yates, *J. Phys. Chem. B* **2005**, *109*, 6061-6068.
- 32 D. C. Hurum, A. G. Agrios, K. A. Gray, T. Rajh, M. C. Thurnauer, *J. Phys. Chem. B* **2003**, *107*, 4545-4549.
- 33 F. Zuo, L. Wang, T. Wu, Z. Zhang, D. Borchardt, P. Feng, *J. Am. Chem. Soc.* **2010**, *132*, 11856-11857.
- 34 K. Suriye, P. Praserttham, B. Jongsomjit, *Appl. Surf. Sci.* **2007**, *253*, 3849-3855.
- 35 M. Zhu, Y. Mi, G. Zhu, D. Li, Y. Wang, Y. Weng, *J. Phys. Chem. C* **2013**, *117*, 18863-18869.
- 36 Y. Mi and Y. Weng, *Sci. Rep.* **2015**, *5*:11482, DOI: 10.1038/srep11482.
- 37 I. Mora-Seró, J. Bisquert, *Nano Lett.* **2003**, *3*, 945-949.
- 38 L. Zhang, Benjamin K. Miller, and Peter A. Crozier, *Nano Lett.* **2013**, *13*, 679-684.

Figures and captions.Table 1. The photocatalytic water splitting of different phases of TiO₂ (anatase, rutile and brookite).

Entry	Samples	Phase	Surface areas (m ² /g)	The amount of gas evolution (μmol/h m ²)		
				H ₂	O ₂	H ₂ /O ₂
1	A1	Anatase	165.8	9.6	0	--
2	A2	Anatase	152.5	10.5	0	--
3	R1	Rutile	14.7	33.8	16.6	2.05
4	R2	Rutile	19.2	23.5	11.5	2.04
5	R3	Rutile	26.3	18.3	8.9	2.07
6	B1	Brookite	26.2	24.8	0	--
7	C-A ^a	Anatase	52.6	6.3	0	--
8	C-R ^a	Rutile	23.4	4.2	2.1	2.04

Reaction conditions: photocatalyst, 50 mg; de-ionized H₂O, 150 mL; 0.2wt% Pt was deposited by in-situ photo-deposition method; Light source, Xenon lamp (300 W); Light intensity, 1000 mW/cm²; Reaction vessel, top-irradiation type; Reaction time, 1 h. ^aC-A: commercial anatase; C-R: commercial rutile.

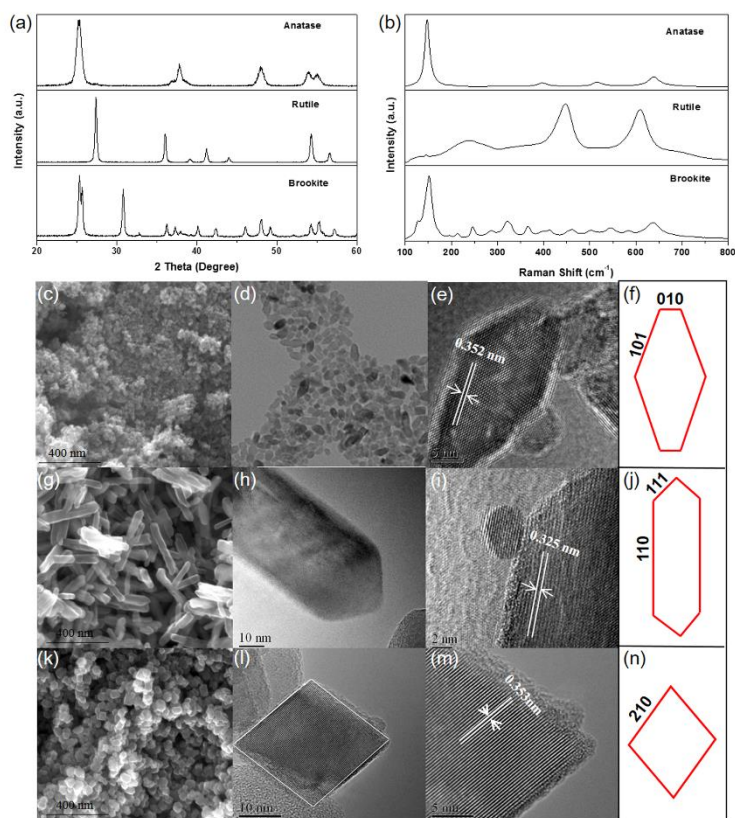


Figure 1. (a) XRD patterns of the anatase, rutile and brookite TiO_2 ; (b) Raman spectra of the anatase, rutile and brookite TiO_2 ; (c-f) SEM and TEM images of anatase TiO_2 ; (g-j) SEM and TEM images of rutile TiO_2 ; (g-j) SEM and TEM images of brookite TiO_2 . A2, R3 and B1 sample in Table 1 were used in these characterizations.

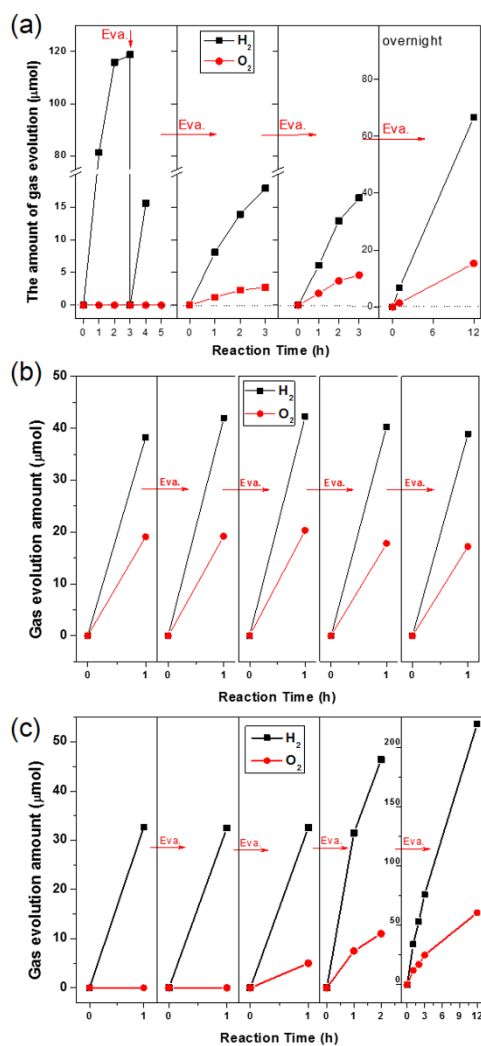


Figure 2. The stability of photocatalytic water splitting for different phases of TiO₂.

(a) anatase ,(b) rutile and (c) brookite.

Reaction conditions: photocatalyst, 50 mg; de-ionized H₂O, 150 mL; cocatalysts: 0.2wt% Pt, photo-deposition method; Light source, xenon lamp (300 W); Light intensity, 1000 mW/cm²; Reaction vessel, top-irradiation type. A2, R3 and B1 sample in Table 1 were used in these characterizations.

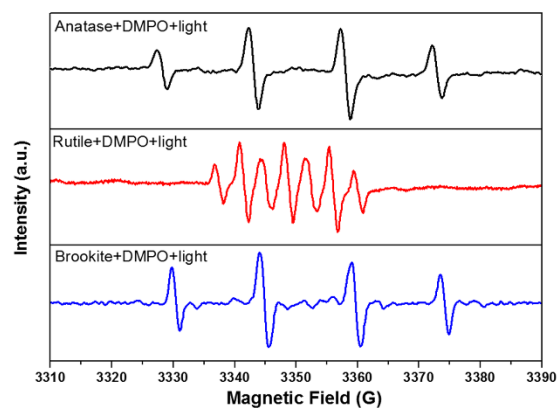


Figure 3. Typical EPR spectra for photocatalytic oxidation of H_2O on different phases of TiO_2 in the presence of DMPO as electron trapping reagent. (a) anatase TiO_2 , (b) rutile TiO_2 and (c) brookite TiO_2 . The signals were collected under the light irradiation. Without the light irradiation, no any signal was detected. Conditions: TiO_2 concentrations, 0.1 mg/ml; DMPO, 5 mM, in argon; irradiation time, 5 min; Test temperature, 298 K; Light source: 100 W Hg lamp, the distance between sample and the light source was fixed to 1.0 m; irradiation time, 5 min. Instrumental settings: microwave power, 20 mW; modulation amplitude, 200 kHz; scan times, 10.

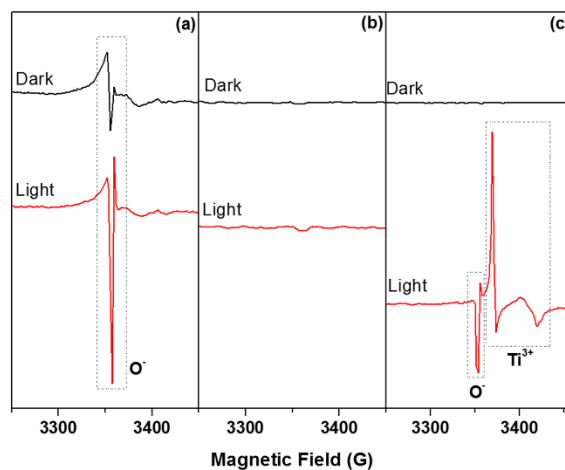


Figure 4. Typical EPR spectra for photocatalytic oxidation of H₂O on different phases of TiO₂ with and without the light irradiation. (a) anatase TiO₂, (b) rutile TiO₂ and (c) brookite TiO₂. The signals were collected after 20 min irradiation. Conditions: 50 mg TiO₂ samples, in argon; Test temperature, 100 K; Light source: 100 W Hg lamp, the distance between sample and the light source was fixed to 1.0 m. Instrumental settings: microwave power, 20 mW; modulation amplitude, 200 kHz; scan times, 10.

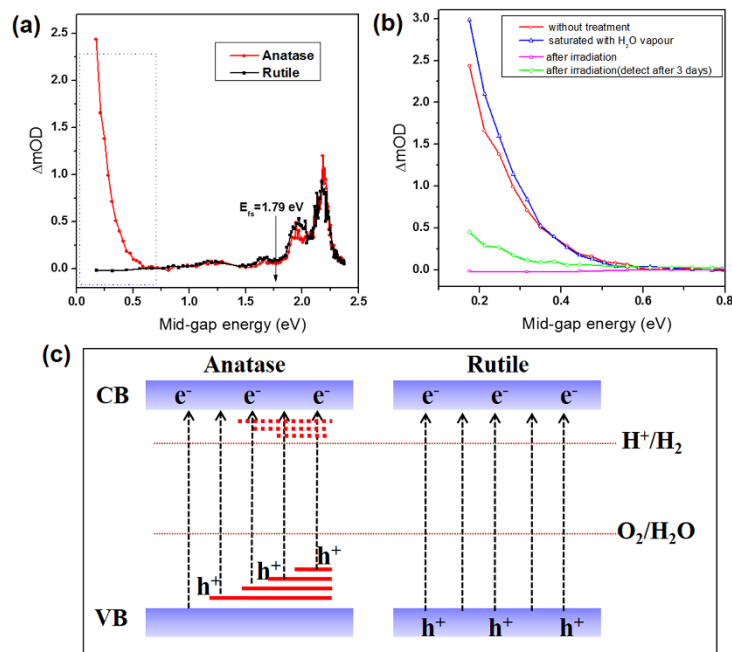
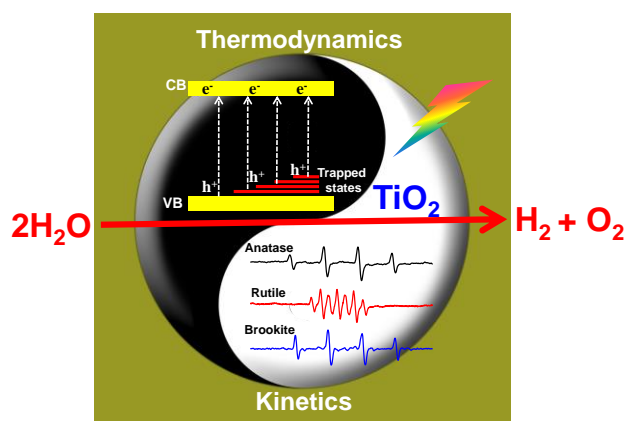


Figure 5. (a) Typical transient IR absorption-excitation energy scanning spectra for anatase and rutile TiO₂. (b) TRIRA-EES for anatase TiO₂ under various conditions: (1) without any treatment; (2) saturated with water vapor; (3) pre-irradiation by 30 mW He-Cd laser (325 nm) for 3.5 hours; (4) pre-irradiation and then recovering for three days after laser treatment. (c) Energy diagram of the trapped electron states for anatase and rutile TiO₂.

Table of Contents.



Photocatalytic overall water splitting on TiO₂-based photocatalyst is determined by both thermodynamics and kinetics simultaneously.

broader context

Photocatalytic overall water splitting to produce H₂ is recognized as a promising strategy for utilization of solar energy. Titanium dioxide (TiO₂) has been widely used as the benchmark semiconductor in photocatalysis, which possesses a suitable band structure and makes the overall water splitting reaction thermodynamically possible. However, achieving overall water splitting on TiO₂-based photocatalysts has remained a long-standing challenge for over 40 years. In this work, we found that the overall water splitting can take place on all three phases of TiO₂ (anatase, rutile and brookite) after a prolonged UV light irradiation. Systematical investigations indicate that both kinetics and thermodynamics factors contributed to unique photocatalytic overall water splitting activity for different phases of TiO₂. This finding will be helpful for understanding why many semiconductors are inactive as overall water splitting photocatalysts despite having thermodynamically suitable band structures for the proton reduction and water oxidation reactions.